UKAEA FUS 464

EURATOM/UKAEA Fusion

Shield design choices for optimum waste management performance

N.P. Taylor

August 2001

EURATOM/UKAEA Fusion Association

Culham Science Centre
Abingdon
Oxfordshire
OX14 3DB
United Kingdom

Telephone: +44 1235 464181
Facsimile: +44 1235 463435

UKAEA Fusion
Working with Europe

Contents

1 Introduction

Neutron activation of materials in a fusion power plant will lead to the generation of a quantity of radioactive material at end of plant life. Some of it may be suitable for recycling and clearance, minimising the quantity categorised as "waste" and needing long-term storage. This waste minimisation requires careful choices at the design stage: the use of low-activation materials in appropriate components, particularly those experiencing a high neutron fluence, and the effective shielding of the large-volume components from significant neutron flux. Studies have shown [1] that such design choices have to optimise the total plant waste volume, for example the use of a low activation material in near-plasma components may result in a higher level of neutron activation elsewhere.

It has previously been noted [2] that the shielding effectiveness of in-vessel materials is particularly important to the total waste volume. The use as blanket structure of certain low activation materials, whose properties derive from their low neutron absorption, lead to higher levels of neutron flux in the vacuum vessel and bulky ex-vessel components. This increases the volume of material that cannot satisfy criteria for clearance, or lengthens the delay before they do so.

The in-vessel shield plays an essential role here, compensating for the lack of shielding provided by a blanket that is relatively transparent to neutrons, reducing activation levels in the vessel and ex-vessel components. In an ideal blanket, every neutron emitted from the plasma would be captured in a reaction with lithium-6 (preferably after a few inelastic scatters in lithium-7), thus producing tritium. But in a practical blanket, even a highly-optimised one, the neutron current from the blanket into the shield is high. An effective shield is therefore bound to become active itself, so the issue of waste management of the shield materials becomes important. Thus the shield design must compromise between the activation of the shield itself and of the vessel and ex-vessel components that it protects. In typical power plant designs the shield materials only marginally satisfy radiological criteria for recyling, so the overall waste performance of the plant is particularly sensitive to these design choices.

Fusion safety studies have identified a further issue with shield materials choice. Analyses of temperature transients in postulated bounding loss-of-coolant accidents [3] revealed that a significant amount of the decay heat to drive such a transient arises in the shield. Furthermore, a reduced-activation austenitic steel with improved long-term activation properties compared with a standard stainless steel was shown to have substantially higher decay heat in the short-term timescale important in accident scenarios [2]. So this aspect of activation behaviour also needs to be taken into account in the materials selection.

A range of issues related to this selection of in-vessel shield materials has been addressed in the studies reported here. The common aspect is the assessment of performance in terms of measures relevant to waste management. This is a departure from the usual objectives of shield design optimisation, which are typically related to minimising materials radiation damage in the vacuum vessel. A common target is the limiting of helium production through (n,α) reactions in vacuum vessel steel to a level that allows the re-welding of the steel throughout the plant life. In contrast, in this report the measures adopted are the potential for materials to satisfy criteria for clearance from regulatory control at some fixed time (50 years) after shutdown, and the gamma dose-rate on a similar timescale, in relation to the limits on materials handling in possible recycling operations.

The issues addressed are:

- For a conventional steel/water shield, optimisation of shield thickness;
- The performance of alternative steels in the steel/water shield;
- A compromise solution to the two goals of low decay heat and low long-term activation properties;
- The viability of shield concepts that have no water content (to avoid the risk of exothermic chemical reactions with beryllium in blanket designs employing this as a neutron multiplier).

These issues are explored in simple neutronic and activation models based on typical power plant design concepts. They are in the spirit of scoping calculations to identify promising concepts or confirm that acceptable solutions exist. There has been no attempt to perform engineering design or to consider detailed shield constructions. These are left for future work as part of power plant conceptual design studies.

2 Computational models

All calculations in this study make use of one-dimensional cylindrical models based on the radial mid-plane build of the power plant designs. These designs are derived from two of the models studied in the second phase of the Safety and Environmental Assessment of Fusion Power (SEAFP-2) [4], although the conclusions of this work should not be sensitive to details such as the plant parameters.

Neutronics modelling has been performed with the ANISN discrete ordinates code [5] using cross sections from the FENDL library [6] in 175 energy groups. A P_3 representation was used for anisotropic scattering and S_8 cylindrical quadrature for the angular flux. Neutron energy multigroup spectra, volume-averaged over each region of interest (see below) were used as input to the FISPACT-99 [7] for activation calculations, using the EAF-99 activation data library [8].

Apart from variations in the shield regions, the radial build of the 1-D models are equivalent to those used in SEAFP-2 for Plant Models 2 and 3 (also known as MINERVA-W and MIVERVA-H) [9]. The former is based on a water-cooled liquid lithium-lead (WCLL) blanket, the latter on a helium-cooled pebble bed (HCPB) with alternate layers of lithium orthoslicate and beryllium pebbles.

An outline of the radial build in the two cases is shown in Table 1. Some of the regions are sub-divided in the neutronics calculations: importantly the first wall is represented as two steel layers with a coolant gap between, and the each blanket is divided into three zones.

Table 1 Outline radial build of 1-D neutronics models

Component	Outer radius, m		Material
	MIVERVA-W	MINERVA-H	
	4.05		void
TF coils	4.80		coil case
	4.81		insulator
	5.59		winding pack
	5.60		insulator
Vacuum vessel	5.71		lead
	5.72		boron carbide
	5.97		316 st.steel + water
	5.99		void
	6.02		316 stainless steel
Inboard shield	6.231	6.303	
Backplate	6.311	6.496	EUROFER + coolant
Coolant manifolds	-	6.624	5 vol.% EUROFER
Inboard blanket	6.926	6.924	homogeneous mixtures (see text)
Inboard first wall	6.951	6.949	EUROFER + coolant
Plasma chamber	11.699	11.699	void
Outboard first wall	11.719	11.726	EUROFER + coolant
Outboard blanket	12.316	12.264	homogeneous mixtures (see text)
Coolant manifolds	-	12.355	5 vol.% EUROFER
Backplate	12.419	12.581	EUROFER + coolant
Coolant feed pipes	-	12.750	5 vol.% EUROFER
Outboard shield	13.250	13.250	
Vacuum vessel	13.30		316 stainless steel
	13.32		void
	13.70		316 st.steel + water
TF coils	14.25		inner coil case
	14.26		insulator
	15.04		winding pack
	15.05		insulator
	15.53		outer coil case

The blanket zones each contain a homogeneous mixture of materials representing the components: $Li_{17}Pb_{83}$ and water for MINERVA-W, Li_4SiO_4 and beryllium for MINERVA-H (helium coolant is represented as a voidage fraction). In both cases the first wall and blanket structural material is assumed to be EUROFER-97. Also not shown in the table is a 2mm layer of beryllium as protective coating on the plasma-facing surface of the first walls, which was included in the calculations.

All neutronic calculations were normalised to a source strength representing a total fusion power of 3 GW. This yields a neutron wall load of 2.4 MW/m^2 at the outboard first wall. In the activation calculations, the fixed components (including the shield under study) is assumed to be exposed to a neutron flux for 25 full-power years.

In the activation calculations, the materials specification assumed for the steels included a full set of impurities. For 316 stainless steel and OPTSTAB these are the same detailed compositions assumed for the SEAFP-2 studies, resulting from the composition optimisation procedure adopted in that assessment [10]. The composition of EUROFER-97 was taken from [11], with an initial set of impurities as quoted in [12] from measurements by the manufacturers of EUROFER-97 samples. As this covered only part of the range of elements that might be present in very low concentration, for those omitted the corresponding levels assumed in SEAFP-2 for the low activation martensitic steel were assumed.

Output from the FISPACT activation calculations includes the nuclide inventory and activity levels at a range of times after shutdown, and a number of derived quantities including decay heat density, contact gamma dose rate and Clearance Index. This Clearance Index is calculated within FISPACT using the IAEA recommended clearance levels for each nuclide [13]. The overall index is the sum over all nuclides of the ratio of the nuclide activity to this clearance level; a Clearance Index of unity or less indicates that the material could be cleared from regulatory control.

In this study the focus is on the effect of the choice of shield materials on waste-related activation parameters in the vessel and ex-vessel components. These have been characterised in most cases by using the following quantities as indicators:

- Contact gamma dose-rate (μSv/hr) at the outboard vacuum vessel 50 years after shutdown;
- Clearance Index of the outboard vacuum vessel material at 50 and 100 years after shutdown;
- Clearance Index of the outboard toroidal field coil steel casing, on the side nearest the plasma, at 50 and 100 years after shutdown.

In addition, the total neutron flux at these locations is noted, and of course results within the shield itself, including decay heat density (W/kg), gamma dose-rate (μSv/hr), and Clearance Index.

All these indicators are on the outboard side, and where shield thickness variations are studied this has been done on the outboard side. Both inboard and outboard shield compositions are kept consistent in the studies of variations in this, but only results on the outboard side are noted here. It can be expected that similar trends would be observed in the inboard shield, although quantitatively different optima may obtain. In practice these may be subject to limits imposed by restricted space for inboard shielding due to the toroidal geometry, as well as possible difficulty in rejection of decay heat from inboard components in postulated loss-of-coolant accidents. From the waste management perspective, it is worth noting that only a small fraction of the total vacuum vessel material volume is in that section of the inboard side where the neutron flux is potentially high.

3 Steel/water shield thickness scoping

3.1 Aim

The nominal dimensions of the in-vessel shields in the plant models used here are based on those adopted for the original SEAFP models [14] and used throughout the various phases of SEAFP studies. On the outboard side, the shield has a thickness of 830 mm, with a composition assumed to be 80% steel and 20% water (by volume). The shield design was based on requirements of limiting radiation damage of the vacuum vessel, and has not been re-optimised as other aspects of the plant design, such as details of the blanket, have been changed. Thus it is valuable to consider an optimisation of the shield thickness, from the point of view of waste management criteria.

3.2 Calculations performed

The MINERVA-W model was used to scope the thickness of the outboard in-vessel shield. The inboard shield was kept of fixed size and not studied. The shields were assumed to be fixed at the nominal composition of 80% (by volume) 316 stainless steel and 20% water coolant. The thickness of the outboard shield was varied in six steps from 63 to 113 cm, as shown in the schematic diagram, Figure 1.

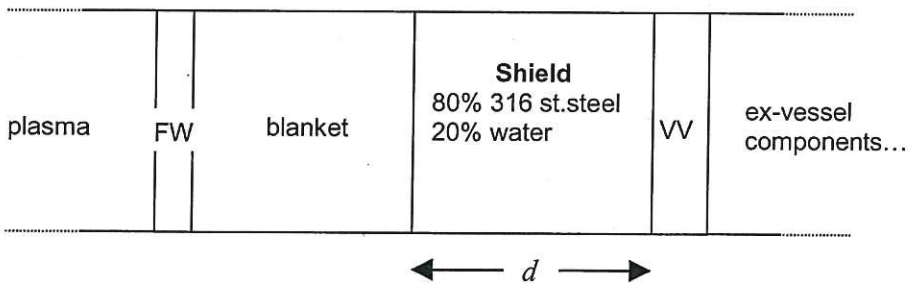

Figure 1 Schematic of shield thickness scoping.
The value of *d* ranges from 63 to 113 cm.

As the dimension *d* is varied, the radial dimensions of the vacuum vessel and all outer components also change, leading to some variation in their volumes.

The shield was sub-divided into 30 radial meshes, grouped into five radial zones. Volume-averaged neutron flux spectra in each of these, as well as in the vacuum vessel, were used as input to FISPACT runs to obtain the activation of the steel material after 25 full-power years irradiation. This provided activation parameters including the contact gamma dose rate and Clearance Index, as a function of time after shutdown and of radial position in the shield.

3.3 Results

The radial variation of Clearance Index (CI) and contact gamma dose-rate, both 50 years after shutdown, are shown in Figures 2 and 3 for all six shield thicknesses. In each case the right-most point represents the result for the vacuum vessel. There are no surprises here, with a linear decrease (on these logarithmic scales) as the thickness is increased, except at the largest thickness where the vacuum vessel result is beginning to flatten off.

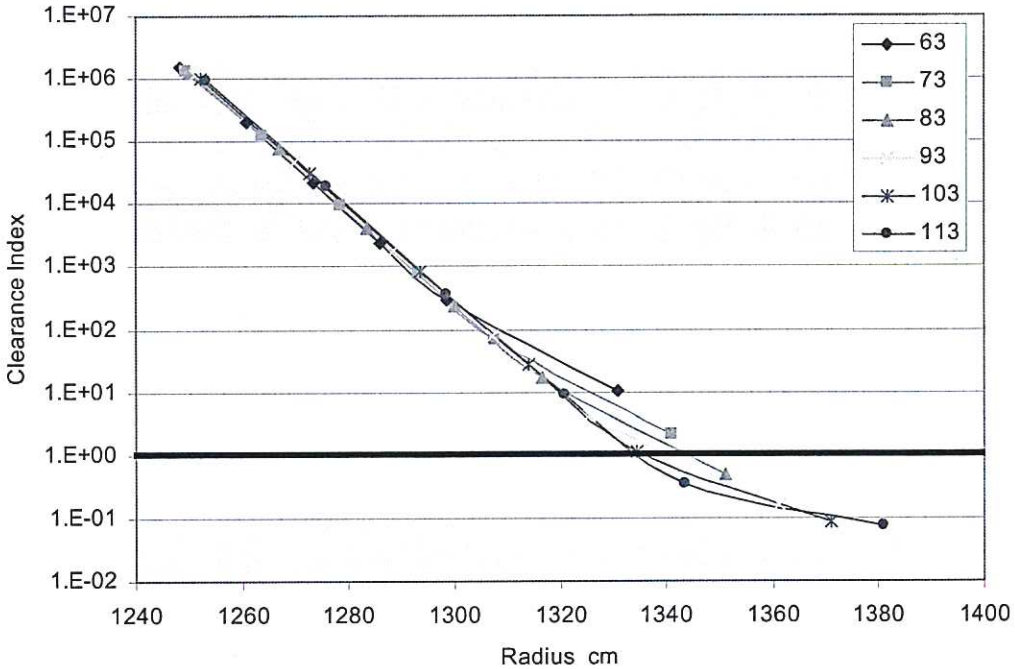

Figure 2 Clearance index (after 50 years) at radial positions in 316 stainless steel/water shields of various thicknesses (63 - 113 cm) **and vacuum vessel**

It is apparent from Figure 2 that if the vacuum vessel is to achieve clearance at this 50 year time (i.e. CI < 1.0 for the right-most point in the line) then a shield thickness of around 80 cm is required. Figure 3 shows that even the thinnest shield would result in a gamma dose-rate at the vessel of less than 10 μSv/hr allowing hands-on operations such as recycling at this time. These results are emphasised by Figure 4, which shows

the two values, gamma dose rate and Clearance Index, for the vacuum vessel material, as a function of the shield thickness. Recall that the vacuum vessel dimensions also vary as the shield thickness is changed.

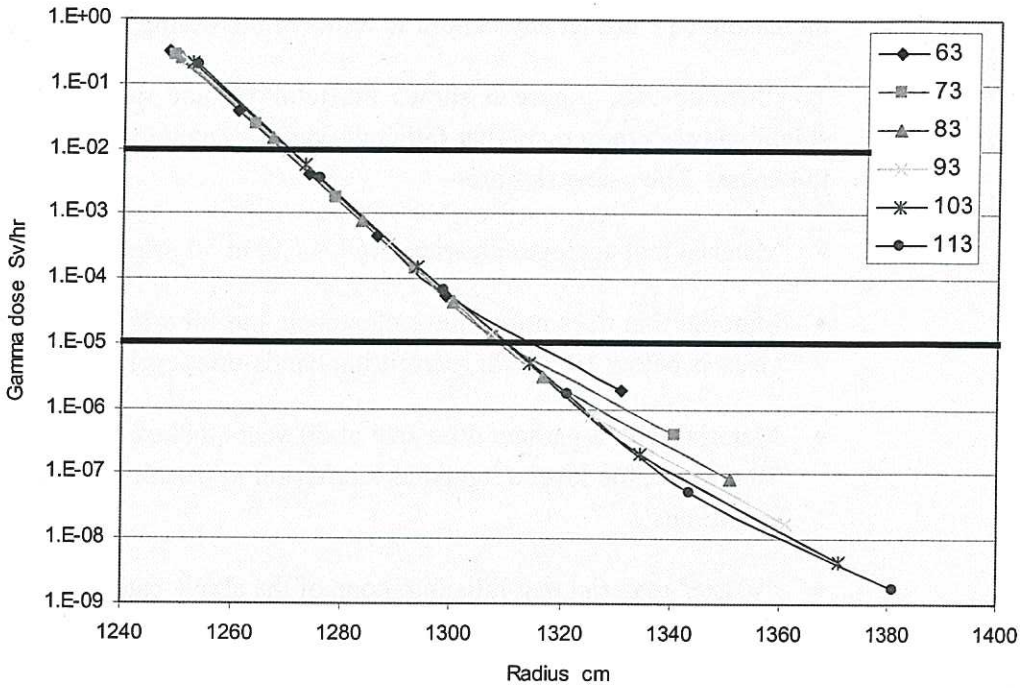

Figure 3 Gamma dose rate (after 50 years) at radial positions in 316 stainless steel/water shields of various thicknesses (63 - 113 cm) **and vacuum vessel**

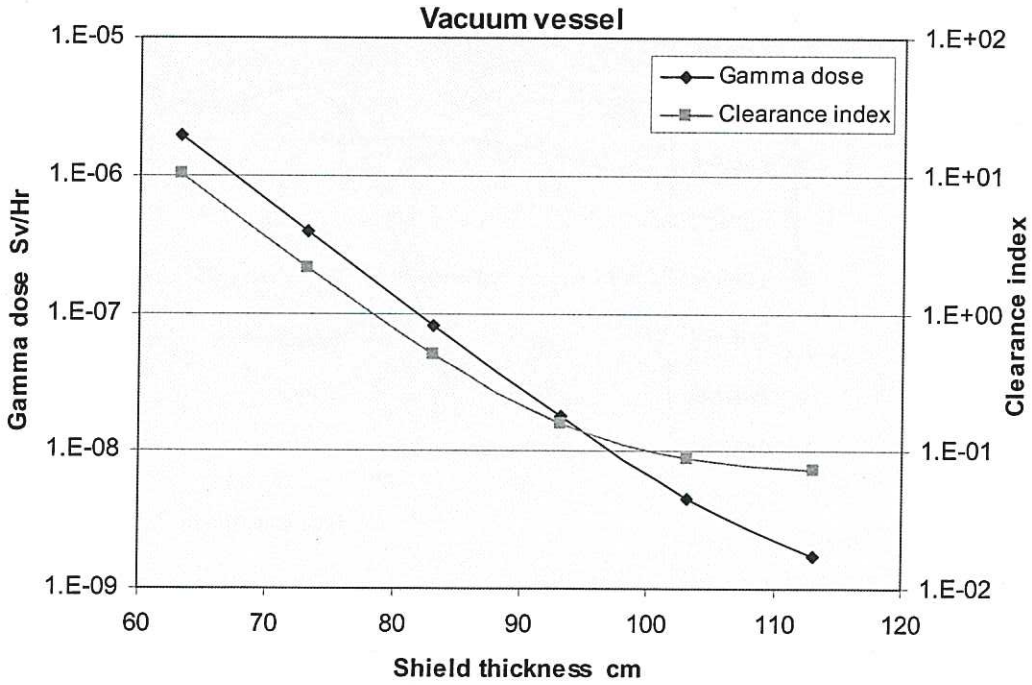

Figure 4 Effect of thickness of steel/water shield on gamma dose and Clearance Index of vacuum vessel material (at 50 years)

As the thickness of the shield is increased, the clearance potential of the vacuum vessel improves (i.e. it could reach a Clearance Index of 1 earlier). But the volume (and mass) of the vessel, and of the shield itself, increases as the square of the radial dimension. So an "optimum" thickness could be regarded as one for which no further increase would attract any benefit in terms of increasing the clearance potential.

To illustrate this, Figure 5 shows the total volume of material from the outboard shield and vacuum vessel that falls into various categories, as a function of the shield thickness. The categories are:

- Material that achieves clearance (CI < 1.0) at 50 years;
- Material that does not achieve clearance, but for which the gamma dose rate at 50 years is below 10 μSv/hr, permitting hands-on recycling;
- Material with a gamma dose rate at 50 years that exceeds 10 μSv/hr, but is below 10 mSv/hr, the level adopted as a criterion to permit recycling by remote handling operations[1];
- "Waste" material that falls into none of the above categories and therefore requires disposal.

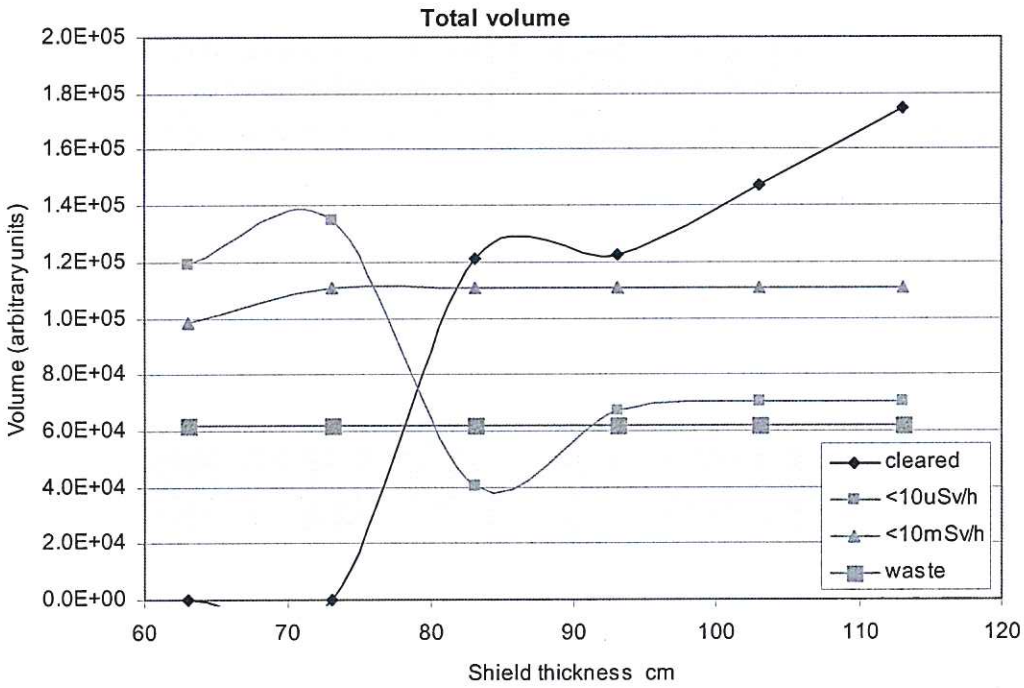

Figure 5 Total shield and VV material in different categories as function of steel/water shield thickness

[1] This limit is under review; current opinion is that it is too conservative and should be set higher.

The first notable result in Figure 5 is that the quantity of waste material requiring disposal (according to the criterion of 10 mSv/hr gamma dose at 50 years) is constant. This is the first 20 cm thickness of the shield, and is not affected by anything at larger radius. Each other line in Figure 5 shows an increase as the thickness increases and more material is introduced above the threshold, until the next limit is reached. For example the purple line, representing hands-on recyclable material, initially increases as the volume of the vacuum vessel material increases, but then at around 75 - 80 cm of shielding it reaches clearance, so all the volume switches to the blue (clearance) line, which sees a sharp rise. Ultimately further shield thickness increases only serve to increase the volume of material in this clearable category.

The optimum point mentioned above is therefore the thickness at which clearance is achieved for the maximum proportion of the material, the hands-on recycling proportion being at a minimum, and the other categories remaining at their invariant values. This point is seen from Figure 5 to be at about $d = 83$ cm. This is the existing value that has been assumed in all previous studies of the MINERVA-W design (also known as SEAFP Plant Model 2), which can therefore be viewed as already optimised. It is, however, a co-incidence that this same value emerges from the present study - the original choice of this dimension was based on different design criteria and in a different plant design.

4 Choice of steel for steel/water shield

4.1 Aim

The calculations reported above in section 3 assumed 316 stainless steel, with water coolant, as the shielding material. In some SEAFP models, an alternative reduced-activation austenitic steel, OPTSTAB, has been assumed. This has lower long-term activation properties, but a high mangenese content leading to increased short-term decay heat (see section 5). It is interesting to compare the shielding performance of these two, using our waste management criteria, along with a low-activation ferritic-martensitic steel, EUROFER, and also, for reference, pure iron with no impurities.

4.2 Calculations performed

The MINERVA-W model was again used for these calculations. A fixed outboard shield thickness of 83 cm was assumed, and a composition of 80% steel and 20% water coolant by volume. In four separate calculations, this "steel" was assumed to be 316 stainless steel, OPTSTAB, EUROFER-97, and pure iron.

As indices of the shielding performance, from the waste management perspective, the gamma dose rate and Clearance Index of the vacuum vessel at 50 years after shutdown were chosen. The Clearance Index of ex-vessel components was also

observed, using as a reference the toroidal field coil steel case (on the side nearest the plasma). FISPACT runs were performed to obtain these quantities, using the neutron flux spectra from the ANISN runs. A further FISPACT run was performed in each case to obtain the decay heat at short times in the zone at the front of the shield (i.e. side nearest the plasma), in view of the interest in this quantity as a potential heat source in postulated loss-of-coolant accidents. Finally FISPACT runs for every radial zone in the shield provided the contact gamma dose rate at 50 years in each case.

4.3 Results

The results for the four cases are summarised in Table 2. A striking feature is that the clearance potential of the coil case is insensitive to the choice of steel in the shield. However the results for the vacuum vessel show significant variation, of up to a factor 2.5.

Table 2 Activation parameters for different materials in steel/water shield

Shield material (+ 20% water)	Gamma dose rate in VV at 50 yr µSv/hr	Clearance index of VV at 50 yr	Clearance index of TF coil case at 50 yr	Decay heat at front of shield W/kg @ 1 hr
316 stainless	0.12	0.69	0.071	0.59
OPTSTAB	0.15	0.82	0.071	1.91
EUROFER	0.24	1.32	0.071	0.341
Pure iron	0.30	1.63	0.071	0.015

On these measures, the shielding performance of 316 stainless steel is slightly better than that of OPTSTAB, and the poor decay-heat characteristics of the latter is noted (this is the topic of section 5, below). But the shielding performance of EUROFER is significantly poorer, and pure iron is even worse. Neither of these could be considered as candidates, unless extra shielding thickness were allowed to compensate for the poor performance. However, no study has been performed here of optimising the steel/water mixture for these two, or of possible combinations with other materials, which could be explored if there were some other incentive for the use of EUROFER or iron. The decay heat produced by either is acceptably low - the iron result is probably artificially low because of the assumed absence of any impurities.

The radial profile of the decay heat at 1 hour is shown for each case (except the pure iron) in Figure 6, and that of the gamma dose rate at 50 years in Figure 7.

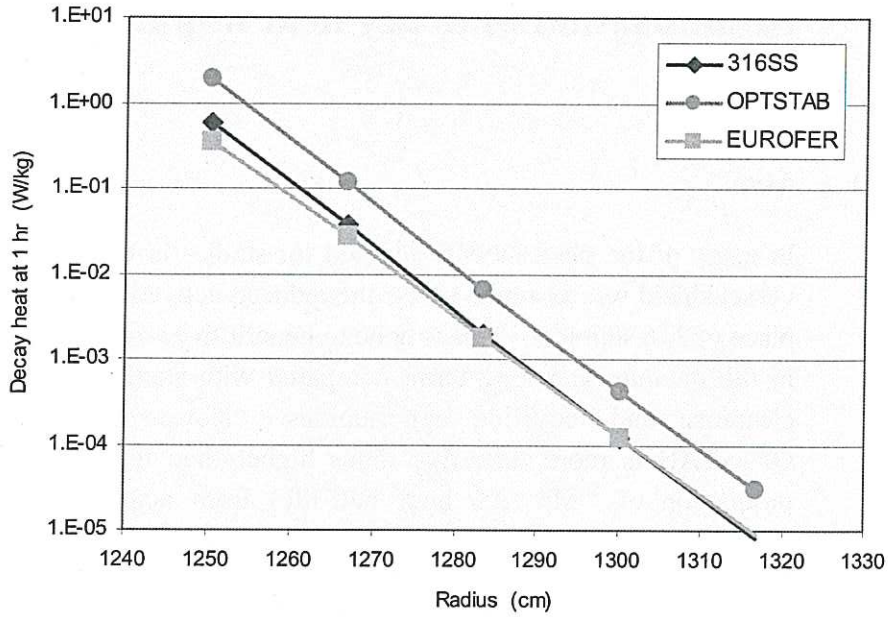

Figure 6 Radial decay heat profile 1 hour after shutdown in steel/water shields of different steel compositions

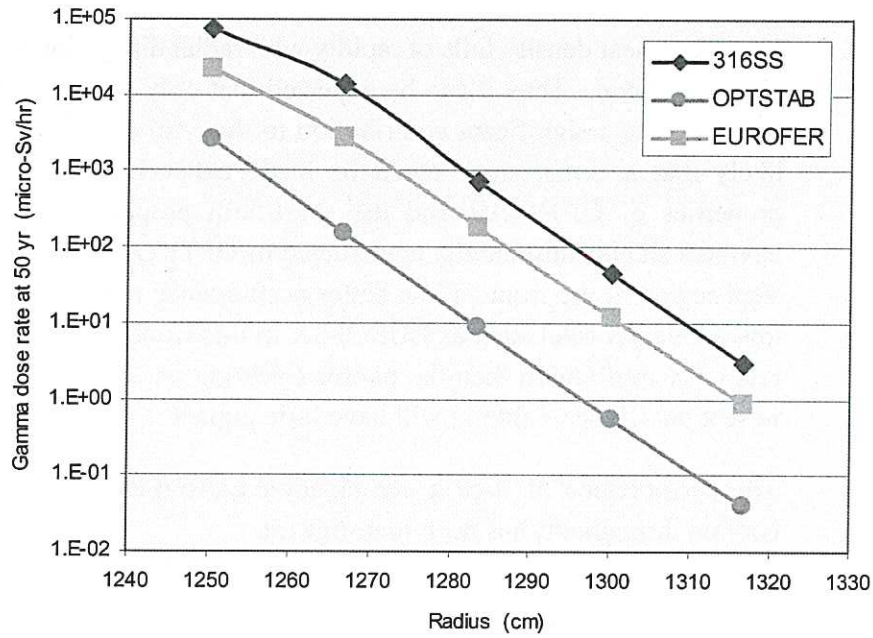

Figure 7 Radial profile of gamma dose rate 50 years after shutdown in steel/water shields of different steel compositions

5 Minimisation of decay heat impact of steel/water shield

5.1 Aim

In many of the plant models adopted for studies in the SEAFP programmes, the in-vessel shield was assumed to use the reduced-activation austenitic steel OPTSTAB in place of 316 stainless. This is done to benefit from the lower activation of OPTSTAB in the medium and long term, compared with standard steels, and leads to earlier clearance and recycling opportunities. However, the manganese content of OPTSTAB is more than five times higher than that of 316 stainless steel. The production of ^{56}Mn (2.6 hour half-life) from neutron capture in ^{55}Mn yields a significant contribution to decay heat in the short term, and the overall decay heat output from OPTSTAB is typically three times that of 316 stainless steel at times up to one month after shutdown [2]. This is of potential importance in postulated loss-of-coolant accidents, in which the decay heat from the front region of the shield augments that in the blanket to drive a temperature transient. The three-fold increase in decay heat from OPTSTAB compared with 316 stainless steel, as seen in Table 2 above, was found in calculations in SEAFP-2 to result in peak temperatures some 120°C higher, in the bounding case of total and prolonged loss of coolant [15].

The decay heat density falls of rapidly with radial dimension into the shield, as seen in Figure 6 above. Thus it can be expected that only a small region at the front of the shield makes a significant contribution to the total decay heat output. It thus seems likely that a compromise could be made between the better long-term activation properties of OPTSTAB and the short-term properties of 316 stainless steel, by having a shield substantially constructed of OPTSTAB, but with a small 316 stainless steel region at the front. Even better performance might be obtained by the use of a low activation steel such as EUROFER in this front portion of the shield - if this is a relatively thin region then the poorer shielding performance of EUROFER (as noted in section 4.3, see Table 2) will have little impact.

The performance of such a combination EUROFER-OPTSTAB shield (with water cooling throughout) has been investigated.

5.2 Calculations performed

The MINERVA-W model was again used for these calculations. A fixed outboard shield thickness of 83 cm was adopted, but the shield was divided into two zones, using EUROFER in the front section and OPTSTAB in the remainder, in each case with 20% water coolant by volume. The boundary between the two sections was considered a variable. This configuration is illustrated schematically in Figure 8.

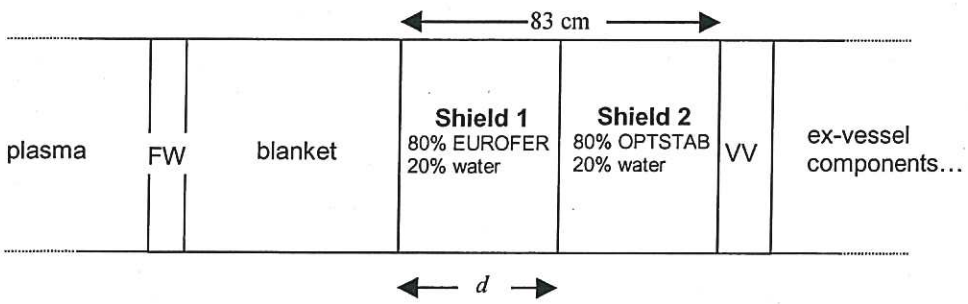

Figure 8 Schematic of combined EUROFER-OPTSTAB shield

To make an initial evaluation of the potential of this concept, and to estimate a suitable value for *d*, the thickness of the front EUROFER portion, use was made of two of the calculations already performed. These are the EUROFER/water and OPTSTAB/water shield cases reported in section 4. The neutron flux spectra from the first six mesh intervals at the front of the shield (each 27.7 mm thick), as well as in five larger zones in the rest of the shield, were used as FISPACT input to obtain the decay heat density in both the EUROFER and OPTSTAB cases. Taking results from selected meshes of each of these two cases enabled the total decay heat to be evaluated for a range of options with different numbers of meshes containing EUROFER or OPTSTAB.

This procedure is approximate, as it ignores the differences in the detail of the effect of EUROFER and OPTSTAB on the neutron energy spectra. But it is adequate to choose a value of *d* to meet some criteria. The criteria adopted was that the total decay heat output from the combined EUROFER-OPTSTAB shield should be the same as that from the standard 316 stainless steel shield, this having already been accepted as allowable. Having in this way selected a value of *d*, a full calculation was then performed with a model representing the combination, to confirm the result without the effect of the approximation.

5.3 Results

The outcome of the calculational process is shown in Figure 9. This shows the total decay heat output from the shield (expressed as the overall average W/kg) as a function of the thickness, *d*, of the EUROFER section at the front. The "Radius" value of the abscissa is the position measured from the axis of the torus, as in the radial build of Table 1. So the leftmost point indicates the decay heat output from a shield entirely constructed of OPTSTAB, the rightmost point that of one entirely of EUROFER (with 20% water coolant by volume in all cases). The broken red line indicates the adopted target value, equivalent to the decay heat output from the "standard" shield of 316 stainless steel.

This plot shows that this target is achieved when the location of the boundary between the EUROFER and OPTSTAB sections is at 1253 cm, equivalent to a EUROFER section thickness $d = 11$ cm.

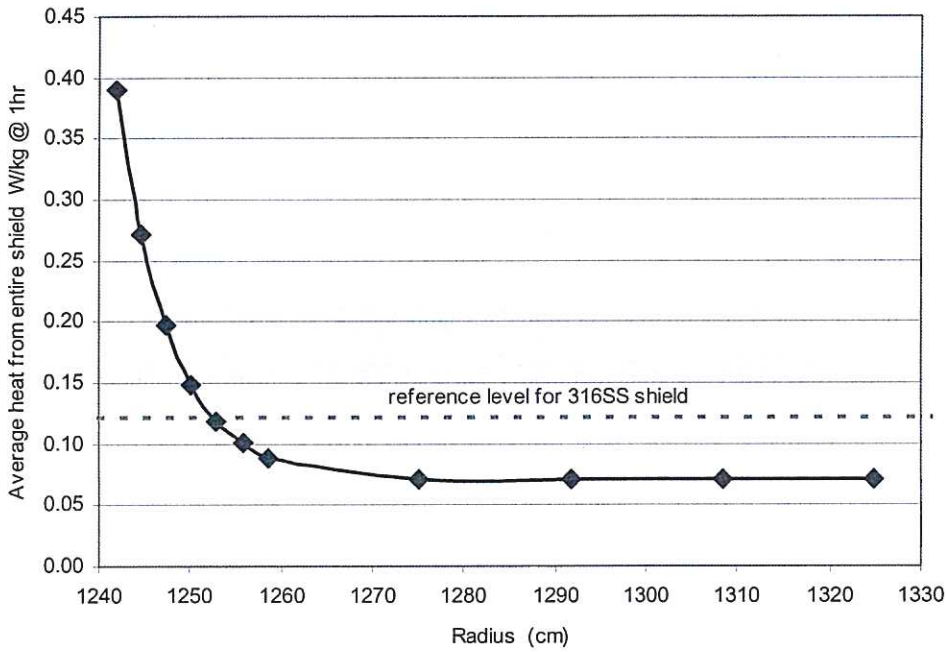

Figure 9 Total decay heat (expressed as average per kg) in combination EUROFER/OPTSTAB and water shield, as function of location of boundary between EUROFER and OPTSTAB

To confirm the effectiveness of this arrangement, a further calculation was performed representing this selected dimension, i.e. with 11 cm of EUROFER followed by 72cm of OPTSTAB (all with 20% water coolant). The inboard shield was assumed to be entirely OPTSTAB/water.

The first important issue is how effective is this combination EUROFER/OPTSTAB as a shield. This can be assessed using the same quantities as in section 4, and these are given in Table 3, which is comparable with Table 2.

Table 3 Shielding performance of combination EUROFER/OPTSTAB shield

Shield material (+ 20% water)	Gamma dose rate in VV at 50 yr µSv/hr	Clearance index of VV at 50 yr	Clearance index of TF coil case at 50 yr	Decay heat at front of shield W/kg @ 1 hr
11 cm EUROFER + 72 cm OPTSTAB	0.15	0.86	0.072	0.72

This shows that the shielding performance is very similar to that of a shield entirely OPTSTAB/water. The last column, decay heat in the front region of the shield, is not directly comparible with the single values in Table 2, as the 11 cm EUROFER region gives a more complex radial profile. The profile of decay heat density for the entire shield is shown in Figure 10, in comparison with those of the standard 316 stainless steel and of the OPTSTAB options. The detail at the front of the shield is plotted in Figure 11, in this case in comparison with the shield constructed entirely of EUROFER or entirely of OPTSTAB. As might be expected, the decay heat density is equivalent to that of the EUROFER shield through the 11 cm EUROFER region, and then rises to be close to the OPTSTAB case for the remainder of the shield.

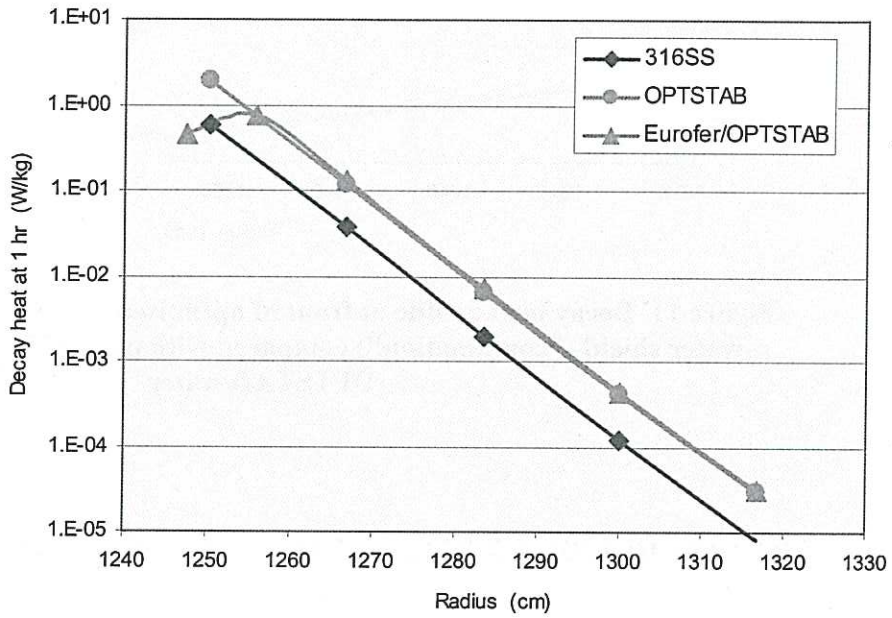

Figure 10 Decay heat profile (at 1 hour) in optimised EUROFER/OPTSTAB and water shield compared with original options

These results show that the concept of a combined EUROFER/water and OPTSTAB/water shield can be effective, and have a modest decay heat output of similar magnitude to that of the 316 stainless steel design assumed in earier accident temperature transient analyses. These conclusions should be regarded as a proof-of-principle, rather than a proposed shield design, because an engineering design of such a combined shield needs to be performed and also thermal analyses of a temperature transient in a postulated loss of coolant, to confirm that the decay heat is indeed at an acceptable level. However, it is important that it has been shown that a solution does exist to the long-standing problem of conflict between requirements for long-term waste management performance and short-term decay heat behaviour.

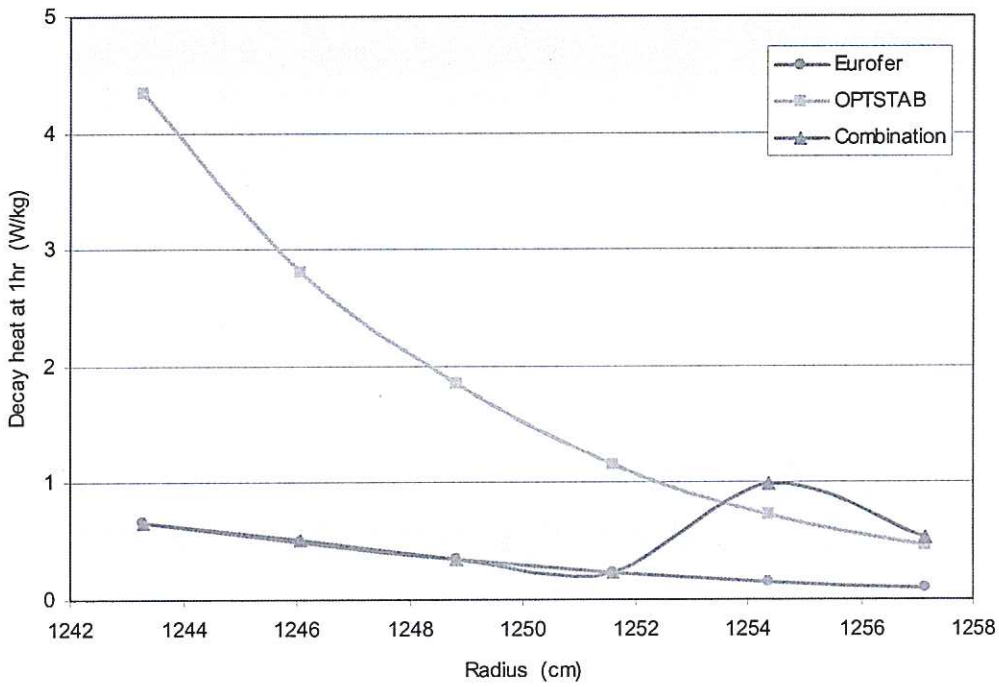

Figure 11 Decay heat profile at front of optimised EUROFER/OPTSTAB and water shield ("combination") compared with pure EUROFER/water and OPTSTAB/water

6 Shield options for designs excluding water

6.1 Aim

The MINERVA-H model, and the equivalent SEAFP Plant Model 3, are based on a helium cooled pebble bed blanket concept that uses beryllium as a neutron multiplier. The beryllium is in the form of a pebble bed, and this occupies the majority of the blanket volume. The blanket is helium-cooled, but in all phases of SEAFP it has been assumed that the shield will be water-cooled steel, similar to that used in MINERVA-W. There is thus the potential for a loss-of-coolant event in this in-vessel shield that leads to a leakage of water (or steam) within the vessel. In principle a sequence could be conceived in which this water comes into contact with the hot beryllium pebbles. The consequent chemical reaction, which is exothermic, could produce large quantities of hydrogen [16] that could further exacerbate the consequences of the accident sequences, for example by challenging confinement barriers.

Although the sequence of failures necessary to bring about such an event is of low probability, the only way of completely avoiding the potential is to exclude water totally from all in-vessel components. This raises the challenge of designing a shield without water. In the water-cooled steel shield, water performs an important neutron

moderation function, as well as acting as the coolant. If an alternative shield is to be gas-cooled, some other neutron moderating material must be introduced. It is important that any replacement shield is of similar size to the existing design, as a significant size increase would increase the dimensions of the vacuum vessel and ex-vessel components, presumably with increased cost.

The purpose of this part of the work is to evaluate some alternative concepts to see whether a viable solution exists, from the perspective of the waste management focus of this study. It must be emphasised that other criteria need to be satisfied, outside the scope of this report, before any of these concepts could be declared as a suitable design option. These include issues such as fabrication, cost, materials properties at high temperature and in a radiation environment, materials compatibility, etc.

As before, only the outboard in-vessel shield is studied here (although for consistency the inboard shield is assumed to have the same composition as the outboard in all cases). The inboard shield may present a greater difficulty, because of the restricted space available. On the other hand, if the inboard shield fails to protect the vacuum vessel as well as the outboard shield this is less important, because the parts of the vacuum vessel on the inboard side that would experience an enhanced neutron fluence is only a small fraction of the total vessel material, owing to the toroidal geometry.

6.2 Calculations performed

The MINERVA-H model has been used for these calculations. In all cases the nominal shield thickness of 50 cm was assumed, but with a variety of shield compositions to represent the alternative options under investigation. These included mixtures of steel and titanium hydride, in a range of proportions, mixtures of steel and zirconium hydride, also in a range of proportions, tungsten carbide, and a mixture of tungsten and titanium hydride. In all cases, a 20% volume void fraction was assumed, to represent the gas coolant channels - any neutronic effect of the coolant itself has thereby been ignored.

In each case investigated, the quantities calculated were as in sections 4 and 5 above, namely the gamma dose-rate at the vacuum vessel 50 years after shutdown, the Clearance Index of the vessel material at the same time, and the Clearance Index of the toroidal field coil steel casing (side nearest the plasma), also at 50 years, as an indicator of the effect on ex-vessel components clearance potential. Additionally, the waste-related activation properties of the shield materials themselves were evaluated, but little can be concluded from these in the absence of a detailed materials specification, including impurities, for the materials chosen.

6.3 Results

6.3.1 Reference case

To enable comparison with a baseline case, a calculation was performed with a standard 80% 316 stainless steel and 20% water (by volume) shield, as assumed in earlier studies of MINVERA-H. The results for the parameters of interest are given in Table 4. The results are relatively poor compared with those for the same shield type in MINERVA-W (first line of Table 2) because of the thinner shield in this plant model (50 cm compared with 83 cm) and because of the greater neutron leakage from the helium-cooled pebble bed blanket.

Table 4 Performance of standard water-cooled shield in MINERVA-H

Shield material	Gamma dose rate in VV at 50 yr µSv/hr	Clearance index of VV at 50 yr	Clearance index of TF coil case at 50 yr	Decay heat at front of shield W/kg @ 1 hr
80% 316 stainless steel + 20% water	15	78	0.22	0.48

It must be emphasised that these results are included in order to provide a benchmark against which to compare the performance of the water-free shield concepts. A water-cooled shield is no longer considered appropriate for a plant model containing beryllium multiplier, as explained above (section 6.1).

In order to illustrate the important neutronic role of water in the effectiveness of this shield, a calculation was performed with the water removed, i.e. with a shield consisting only of 316 stainless steel (and 20% void fraction). The activation of the vacuum vessel increased by a factor of over 200, with a gamma dose rate of 3160 µSv/hr and a clearance index of 16,200, both at 50 years cooling. This confirms that the introduction of some neutron moderating material is essential.

6.3.2 Hydrides

Metal hydrides provide a high density of hydrogen and thus good neutron moderation performance. A pure metal hydride shield was assumed to be difficult to fabricate and costly, so combinations with 316 stainless steel have been investigated. These were represented as homogeneous mixtures of steel and hydride, in a range of proportions, although in a full design some form of layering would presumably be done.

The two hydrides chosen were titanium hydride and zirconium hydride. In both cases these were assumed to have the full hydrogen content (i.e. TiH_2 and ZrH_2) although practical compositions may be lower. It is recognised than an issue with these hydrides is the potential for decomposition at high temperatures, as might be

experienced in an accident involving loss of cooling. This would have to be thoroughly investigated by analyses if the option is selected. It is likely that zirconium hydride would be superior to titanium hydride in this regard.

For each hydride, a range of mixtures with steel was investigated, from 10% hydride, 70% steel and 20% void (by volume) to 40% hydride, 40% steel, 20% void. As noted above, the void fraction was constant at 20% by volume to represent coolant channels. The results are presented in Figures 12 - 15.

Figure 12 shows the two measures in the vacuum vessel, both gamma dose rate and Clearance Index showing the same behaviour as the TiH_2 content is varied. Above about 20% by volume, further improvement is modest. A performance equivalent to that of the standard 316 stainless steel and water shield (Table 4) is achieved at about 25%.

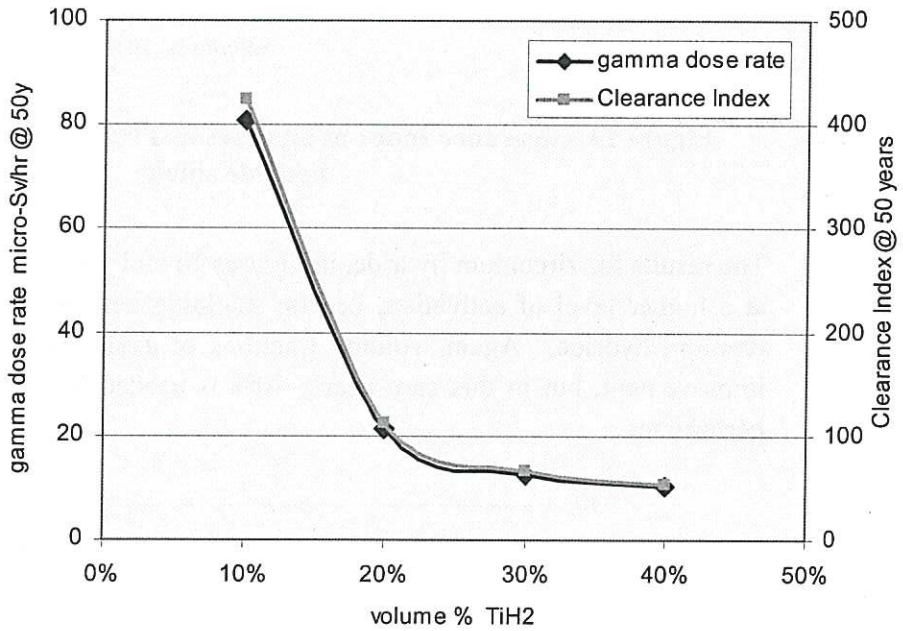

Figure 12 Gamma dose rate and Clearance Index at 50 years in vacuum vessel with steel/titanium hydride shield

The Clearance Index in the toroidal field coil case, plotted in Figure 13, shows little variation, although more than in the variations of steel/water shield in Table 2. It is interesting to note a shallow minimum in the CI at a titanium hydride content in the shield around 25%.

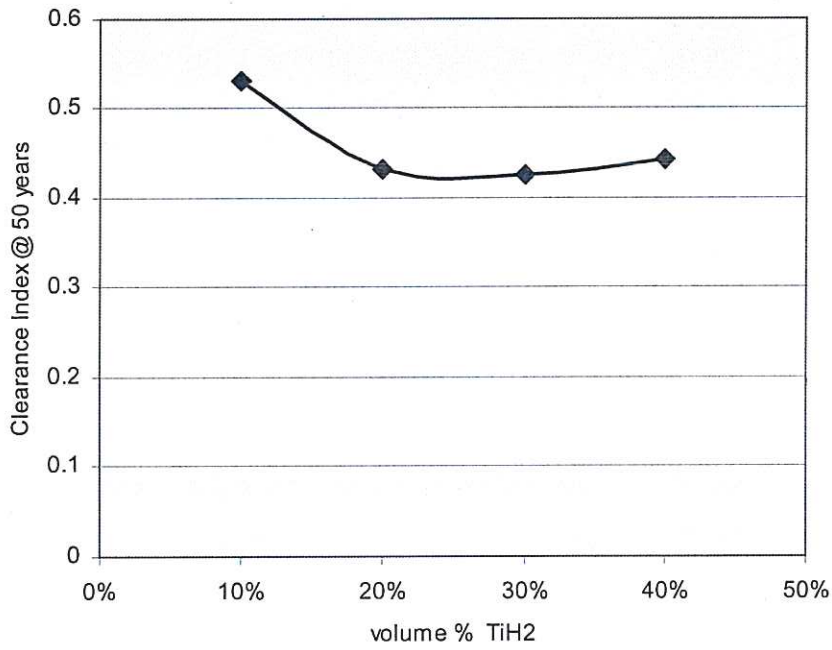

Figure 13 Clearance Index at 50 years in TF coil case with steel/titanium hydride shield

The results for zirconium hydride, in Figures 14 and 15, show the same behaviour, but at a higher level of activation, i.e. the shielding performance is a little poorer than titanium hydride. Again, volume fractions of ZrH_2 above 20% show diminishing improvement, but in this case nearly 40% is needed to match the steel/water shield performance.

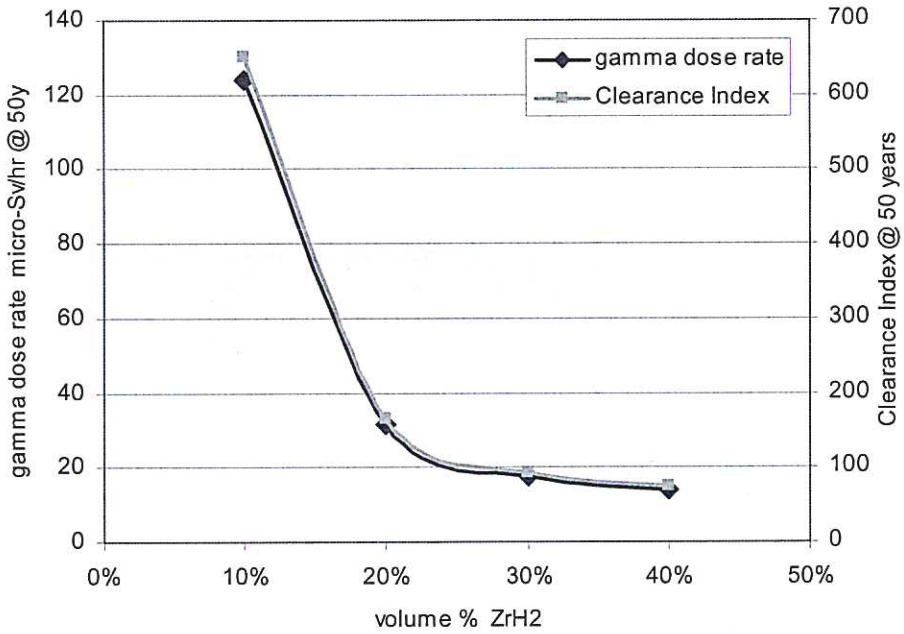

Figure 14 Gamma dose rate and Clearance Index at 50 years in vacuum vessel with steel/zirconium hydride shield

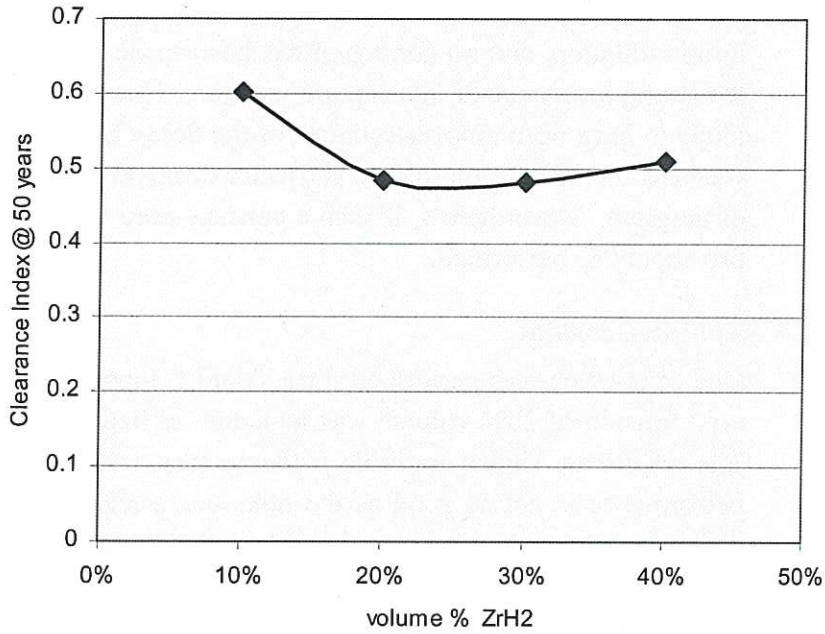

Figure 15 Clearance Index at 50 years in TF coil case with steel/zirconium hydride shield

6.3.3 Tungsten with titanium hydride

A single calculation was performed to assess the use of tungsten in place of stainless steel in these hydride shields. This represented a mixture of 60% tungsten, 20% titanium hydride, and 20% voidage (for the coolant channels), by volume. The results are given in Table 5, which shows a performance better than any of the stainless steel and hydride cases. Although not calculated, it could be anticipated that an alternative of tungsten with zirconium hydride would also give adequate performance. However, the waste-related activation properties of the shield material itself has not been assessed, owing to the lack of information about impurity levels.

Table 5 Performance of a tungsten/titanium hydride shield

Shield material	Gamma dose rate in VV at 50 yr µSv/hr	Clearance index of VV at 50 yr	Clearance index of TF coil case at 50 yr	Decay heat at front of shield W/kg @ 1 hr
60% tungsten + 20% TiH_2	4.3	22	0.16	0.30

Assessing the decay heat from tungsten in this case is important, as it might have been expected that a high level would result. But the result at the front of the shield, 0.3 W/kg after 1 hour, is actually lower than that in the steel/water shield, 0.48 W/kg. This could be because the neutron spectrum at this location has relatively small low-energy component, which is the origin of ^{186}W production by radiative capture in

^{185}W. It should be noted that neutron cross sections used in these calculations are infinite-dilution, and no correction has been made for the effects of self-shielding in the strong resonance of this capture reaction. However, the effect of this omission is likely to have been an over-estimate of the decay heat rate, so strengthens rather than weakens the conclusion that no particular decay heat problem is presented by the use of tungsten. Nevertheless, if such a concept were to be adopted, a thorough study of this should be performed.

6.3.4 Tungsten carbide

One calculation was performed for a shield composed solely of tungsten carbide. A void fraction of 20% volume was included, as before, to represent coolant channels. The results are shown in Table 6 (decay heat was not assessed in this case). The performance is not as good as the reference steel/water shield, with vacuum vessel activation about doubled, but is still in the range that could be considered as an alternative candidate if necessary, and if some increased shielding thickness could be tolerated.

Table 6 Performance of a tungsten carbide shield

Shield material	Gamma dose rate in VV at 50 yr µSv/hr	Clearance index of VV at 50 yr	Clearance index of TF coil case at 50 yr
80% tungsten carbide	32	160	0.15

7 Conclusions

Simple one-dimensional neutronics and activation models have been used to perform scoping calculations for a number of concepts for the in-vessel shield of a tokamak power plant. The aim has been optimisation of performance with respect to activation parameters of importance to waste management, in particular the potential for clearance and recycling of the vacuum vessel material and ex-vessel components. The main conclusions are:

- For the MINERVA-W, the optimum thickness of a 316 stainless steel and water shield (80%/20% by volume) is 83 cm, which is co-incidentally the dimension assumed in existing models.
- OPTSTAB is an alternative to stainless steel in the steel/water shield for MINERVA-W, however the martensitic steel EUROFER-97 is less effective, and pure iron is poorer still.

- In a shield based on OPTSTAB and water, there is increased decay heat compared with 316 stainless steel. However this can be avoided by including a small region of low-activation steel at the front of the shield - an 11 cm thick zone of EUROFER-97 (with water cooling) was found to be adequate.

- Alternatives to the steel/water shield have been investigated for plant designs in which water must be entirely excluded, to avoid the potential for chemical reactions with beryllium multiplier. A mixture of stainless steel and either titanium or zirconium hydride, cooled by helium gas, was found to be adequate (TiH_2 being a little more effective than ZrH_2). However there may be other factors, especially the potential for hydride decomposition at high temperature, that present difficulties. Replacing the steel by tungsten in these mixtures with hydride gives improved performance, and the decay heat level is likely to be acceptable. A helium-cooled tungsten carbide shield has performance that falls short of targets.

8 Acknowledment

This work was funded by the UK Department of Trade and Industry and by EURATOM.

9 References

[1] D.A. Petti, K.A. McCarthy, N.P. Taylor, C.B.A. Forty, R.A. Forrest, "Re-evaluation of the use of low activation materials in waste management strategies for fusion", Fusion Eng. Design 51-52 (2000) 435-444.

[2] N.P. Taylor, C.B.A. Forty, D.A. Petti and K.A. McCarthy, "The impact of materials selection on long-term activation in fusion power plants", J. Nucl. Materials 238-287 (2000) 28-34.

[3] N.P. Taylor, I. Cook, C.B.A. Forty, W.E. Han, P. Taylor, "SEAFP-2 bounding accident analyses", Fusion Eng. Design 48 (2000) 419-433.

[4] I. Cook, G. Marbach, L. DiPace, C. Girard, P. Rocco, N.P. Taylor, "Results, conclusions and implications of the SEAFP-2 programme", Fusion Eng. Design 51-52 (2000) 409-417.

[5] W.W. Engle jr., "A Users' Manual for ANISN, a One-dimensional Discrete Ordinates Transport Code with Anisotropic Scattering", Oak Ridge Gaseous Diffusion Plant report K-1693 (1967).

[6] A.B. Pashchenko and H. Weinke, "FENDL/E-2.0: Evaluated nuclear data library of neutron-nucleus interaction cross sections and photon production cross sections and photon-atom interaction cross sections for fusion applications, Summary documentation", IAEA-NDS-175 (1998).

[7] R.A. Forrest and J-Ch. Sublet, "FISPACT-99: User manual", UKAEA report UKAEA-FUS-407 (1998).

[8] J-Ch. Sublet, J. Kopecky and R.A. Forrest, "The European Activation File: EAF-99 cross section library", UKAEA report UKAEA-FUS-408 (1998).

[9] N.P. Taylor, I. Cook, "Description of plant models, blankets and structural materials", UKAEA report SEAFP2/5.1/UKAEA/1 (March 1997).

[10] C.B.A. Forty, "Compositional optimisation of SEAFP-2 materials", UKAEA report SEAFP2/4.11/UKAEA/4 (August 1998).

[11] E. Daum and U. Fischer, "Long-term activation potential of the steel EUROFER as structural material of a demo breeder blanket", Fusion Eng. Design 49-50 (2000) 529-533.

[12] M. Pillon, "Further measurements on EUROFER 97 using low background HPGe detector", ENEA Frascati report EFF-DOC-778 (May 2001).

[13] IAEA "Clearance levels for radionuclides in solid materials: application of exemption principles", interim report for comment, IAEA TECDOC-855, Vienna, January 1996.

[14] J. Raeder, I. Cook, F. H. Morgenstern, E. Salpietro, R. Bünde, E. Ebert, "Safety and Environmental Assessment of Fusion Power (SEAFP): report of the SEAFP project", EURFUBRU XII-217/95. Brussels: European Commission, 1995.

[15] N.P. Taylor, C.B.A. Forty and W.E. Han, "Accident analyses for variations of SEAFP-2 Plant Models", UKAEA report SEAFP2/5.1/UKAEA/9 (September 1998).

[16] F. Druyts and P. Van Iseghem, "Thermogravimetric analysis of the beryllium/steam reaction", Fusion Eng. Design, 51-52 (2000) 499-503.